Ab initio study on the hydrogen desorption from MH–NH_3 (M = Li, Na, K) hydrogen storage systems

A. Yamane,[1,a)] F. Shimojo,[2] K. Hoshino,[1] T. Ichikawa,[3,4] and Y. Kojima[3,4]
[1]*Graduate School of Integrated Arts and Sciences, Hiroshima University, Higashi-Hiroshima, 739-8521, Japan*
[2]*Graduate School of Science and Technology, Kumamoto University, Kumamoto, 860-8555, Japan*
[3]*Graduate School of Advanced Sciences of Matter, Hiroshima University, Higashi-Hiroshima, 739-8530, Japan*
[4]*Institute for Advanced Materials Research, Hiroshima University, Higashi-Hiroshima, 739-8530, Japan*

(Received 19 October 2010; accepted 14 February 2011; published online 29 March 2011)

The hydrogen storage system LiH + NH_3 ↔ $LiNH_2$ + H_2 is one of the most promising hydrogen storage systems, where the reaction yield can be increased by replacing Li in LiH with other alkali metals (Na or K) in order of Li < Na < K. In this paper, we have studied the alkali metal M (M = Li, Na, K) dependence of the reactivity of MH with NH_3 by calculating the potential barrier of the H_2 desorption process from the reaction of an M_2H_2 cluster with an NH_3 molecule based on the *ab initio* structure optimization method. We have shown that the height of the potential barrier becomes lower in order of Li, Na, and K, where the difference of the potential barrier in Li and Na is relatively smaller than that in Na and K, and this tendency is consistent with the recent experimental results. We have also shown that the H–H distance of the H_2 dimer at the transition state takes larger distance and the change of the potential energy around the transition state becomes softer in order of Li, Na, and K. There are almost no M dependence in the charge of the H atom in NH_3 before the reaction, while that of the H atom in M_2H_2 takes larger negative value in order of Li, Na, and K. We have also performed molecular dynamics simulations on the M_2H_2–NH_3 system and succeeded to reproduce the H_2 desorption from the reaction of Na_2H_2 with NH_3. © *2011 American Institute of Physics*. [doi:10.1063/1.3562122]

I. INTRODUCTION

To realize on-board hydrogen storage for transportation systems, we have to develop a hydrogen storage system with high speed, high reversibility, and high capacity both per volume and per weight. For these purposes, hydrogen storage systems based on light elements have been studied extensively, since they can realize high capacity both per volume and per weight.[1,2] One of the most promising candidates based on light elements is lithium–nitrogen–hydrogen (Li–N–H) reversible system.[3]

The hydrogen storage system based on lithium hydride (LiH) and ammonia (NH_3)

$$\mathrm{LiH(solid)} + \mathrm{NH_3(gas)} \leftrightarrow \mathrm{LiNH_2(solid)} + \mathrm{H_2(gas)} \qquad (1)$$

is an efficient Li–N–H hydrogen storage system which stores about 8.1 mass% of H_2.[4] The hydrogen desorption reaction of this system is exothermic [$\Delta H = 50 \pm 9$ kJ/mol (Ref. 5)], ultrafast,[6] and proceeds at room temperature, and the reverse reaction also proceeds at relatively low temperature and pressure (below 300 °C, 0.5 MPa H_2 flow).[7] One of the advantages of this system is to use NH_3 as the hydrogen storage material. Since NH_3 contains about 17.6 mass% of hydrogen and is liquefied easily, we can regard NH_3 as an excellent hydrogen storage material. In this system, since both NH_3 before the reaction and H_2 after the reaction are gas phase, we can control the hydrogen absorption and desorption by adjusting the partial pressures of NH_3 and H_2.

On the other hand, the reactivity of as-prepared LiH with NH_3 is not so high, and the reaction yield of LiH with 0.5 MPa NH_3 for 24 h with a molar ratio of NH_3/Li = 1 is about 12%.[8] This situation can be improved by ball-milling the LiH, and the reaction yield of LiH*, where the asterisk denotes that the sample is ball-milled, with NH_3 for 24 h is about 53%.[8] The reaction yield can also be increased by replacing Li in LiH* with other alkali metals. The reaction yields of NaH* and KH* with NH_3 for 24 h are about 60% and 100%, respectively.[8] These results indicate that the reactivity of the alkali metal hydrides (MH) with NH_3 increases in order of Li < Na < K.

The dehydrogenation reactions of alkali metal amidoboranes MNH_2BH_3 (M = Li, Na) (Ref. 9) and alkali metal borohydrides MBH_4 (M = Li, Na, K) (Refs. 10 and 11) also show the alkali metal dependence. The experimental hydrogen desorption temperature of $NaNH_2BH_3$ is lower than that of $LiNH_2BH_3$.[9] On the other hand, the experimental hydrogen desorption temperature of MBH_4 increases in order of Li < Na < K, i.e., the reactivity decreases in order of Li > Na > K.[10,11]

In our previous studies,[12] we have performed *ab initio* molecular dynamics (MD) simulations on the reaction of a Li_2H_2 cluster with an NH_3 molecule and reproduced the H_2 desorption, where we used the Li_2H_2 cluster as a model corresponding to extremely disordered LiH surface, since highly periodic clean surface of LiH could not easily react with NH_3. We have shown that the H_2 molecule is formed from $H^{\delta-}$

a)Electronic mail: yamane@minerva.ias.hiroshima-u.ac.jp.

in the Li_2H_2 cluster and $H^{\delta+}$ in the NH_3 molecule, which is consistent with the assumed process in previous theoretical studies.[13,14] We have also shown that the reaction model can qualitatively reproduce the experimental hydrogen desorption profile[15] from LiD and $LiNH_2$.

The purpose of this paper is to reveal the M (M = Li, Na, K) dependence of the reactivity of the H_2 desorption from the reaction of MH with NH_3

$$MH(solid) + NH_3(gas) \rightarrow MNH_2(solid) + H_2(gas) \qquad (2)$$

by performing *ab initio* calculations on the systems consisting of an M_2H_2 cluster and an NH_3 molecule.

In Sec. II, we explain the two theoretical approaches employed in this paper, i.e., *ab initio* structure optimization calculation and *ab initio* MD simulation. We also give the details of our model system. In Sec. III, the results and discussions are shown. In Sec. III A, the potential barriers, the atomic configurations, and the atomic charges obtained by *ab initio* structure optimization calculation are shown and the results of dynamical reaction processes studied by *ab initio* MD simulation are shown in Sec. III B. Finally, a brief summary is given in Sec. IV.

II. METHOD

We have performed *ab initio* structure optimization calculations and MD simulations based on the density functional theory,[16–22] where the Kohn–Sham energy functional is minimized by the preconditioned conjugated gradient method[18,22] and the generalized gradient approximation by Perdew-Burke-Ernzerhof (Ref. 23) is used for the exchange-correlation energy. The interaction between valence electrons, $(1s)^1$, $(2s)^1$, $(3s)^1$, $(4s)^1$ electron of H, Li, Na, and K, respectively, and $(2s)^2(2p)^3$ electrons of N, with ions are treated by the projector augmented wave method.[24,25] The cutoff energies for the plane wave expansions of the wave function and pseudocharge density are 476 and 2040 eV, respectively, and k-point sampling in the Brillouin zone is done only for Γ-point. The atomic charges of each atom during the reaction process are calculated by the Mulliken analysis.[26]

The simulation cell of our calculations is a rectangular parallelepiped with the periodic boundary condition, and its size is (x, y, z) = (16.616 Å, 8.308 Å, 8.308 Å), (19.2736 Å, 9.6368 Å, 9.6368 Å), and (23.056 Å, 11.528 Å, 11.528 Å) for Li, Na, and K, respectively. The initial configuration for Li is shown in Fig. 1. The M_2H_2 cluster is put to be a square and NH_3 is put to be directed N(7) to M(5). The M_2H_2 cluster and N(7) are placed on the same x–y plane, and N(7), H(2), M(5), and M(6) are placed on the same x–z plane. The Li–H distance in Li_2H_2 is 2.077 Å, which is the Li–H distance of bulk LiH.[12] The Na–H and K–H distances in Na_2H_2 and K_2H_2 are 2.409 Å and 2.882 Å, respectively, which are also the M–H distances of bulk MH as shown in Sec. III. We also set the M(5)–N(7) distance to be 2.077, 2.409, and 2.882 Å for M = Li, Na, and K, respectively. Notice that these initial configurations are not the configuration at the energy minimum before the reaction (top row in Fig. 3).

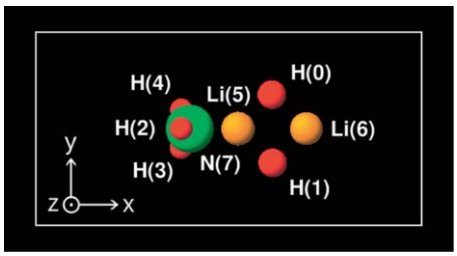

FIG. 1. Initial configuration of the Li_2H_2 cluster and NH_3. H(0), H(1), Li(5), Li(6), and N(7) are placed on the same plane.

In this paper, we have studied the H_2 desorption processes by the structure optimization calculations and the MD simulations, which we explain briefly below.

The structure optimization calculations (Sec. III A) have been performed by the projected Velocity Verlet method.[27] At first, we performed MD simulations to realize the atomic configuration before the reaction at finite temperature (see Ref. 12 and Sec. III B), and then performed the structure optimization to obtain the most stable atomic configuration with the energy minimum. After we obtained the most stable structure, in which a H atom in M_2H_2 and a H atom in NH_3 get close to each other, we made the distance of these two H atoms (d_{H-H}) closer step by step and performed the structure optimization at each d_{H-H}. The energy of the *most stable structure* increases with decreasing d_{H-H}, and has a maximum value at some d_{H-H}. When the energy of the *most stable structure* begins to decrease with further decrease of d_{H-H}, the structure optimization is performed without fixing d_{H-H} again to obtain the most stable structure with the energy minimum after the reaction.

The MD simulations (Sec. III B) have been performed under the constant number of atoms, constant volume, and constant temperature ensemble with the temperature control by Nosé–Hoover thermostat.[28–30] We set the time step to be 0.48 fs (about 1/20 of the period of N–H stretching) and performed MD simulations up to 30 000 steps (14.4 ps). The velocity scalings

$$\mathbf{v}_i' = \mathbf{v}_i \cdot \left(\frac{3Nk_BT}{\sum_{i=1}^{N} m_i |\mathbf{v}_i|^2} \right)^{1/2} \qquad (3)$$

are done 25 times at every 20 time steps at the beginning of the simulations, where $\mathbf{v}_i'$, $\mathbf{v}_i$, and m_i are the velocity before the scaling, the velocity after the scaling, and the mass of ith atom, respectively, and N is the number of atoms, k_B is Boltzmann constant, and T is the required temperature. Since the present system is an isolated small system consisting of eight atoms, we can regard that the system quickly reaches to the equilibrium. The temperatures of the simulations are 700 and 1000 K. Since we perform MD simulations at temperatures higher than room temperature, we fixed the positions of the Li atoms to focus our attention on the behavior of N and H atoms.[12]

III. RESULTS AND DISCUSSIONS

At first, we have performed *ab initio* calculations on bulk MH (M = Na, K), where the crystalline structure of the alkali

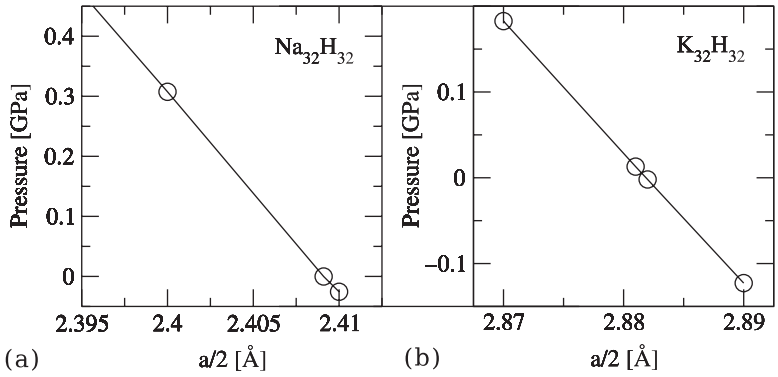

FIG. 2. M–H distance $a/2$ (half of the lattice constant a) and pressure of $M_{32}H_{32}$ for (a) M = Na and (b) M = K.

metal hydrides is NaCl structure.[31] We took 2×2×2 unit cells as the simulation cell, i.e., the system is $M_{32}H_{32}$.

In Fig. 2 we show the pressure of $M_{32}H_{32}$ as a function of the M–H distance $a/2$ (half of the lattice constant a) for (a) M = Na and (b) M = K. From the figure, we can see that the pressure becomes almost zero at $a/2 = 2.409$ and 2.882 Å for M = Na and K, respectively. The bulk moduli of NaH and KH are evaluated as 14.4 and 25.9 GPa, respectively, and the bulk modulus of NaH agrees well with the previous studies (Ref. 32 and references therein). For M = Li, $a/2$ is 2.077 Å and the bulk modulus is 35.3 GPa.[12]

A. Reaction process by structure optimization calculation

1. Snapshots

In Fig. 3 we show the snapshots of the reaction processes of M_2H_2 with NH_3 obtained by the structure optimization calculations. The left, center, and right columns show the atomic configurations for M = Li, Na, and K, respectively. The top, middle, and bottom rows show the atomic configurations corresponding to those of the energy minimum before the reaction (M_2H_2–NH_3), the energy maximum during the reaction (transition state), and the energy minimum after the reaction (M_2HNH_2–H_2), respectively. From Fig. 3, we can see that these three systems show the similar reaction processes, i.e., NH_3 molecule stays on an M atom directing its N atom to M, and a H atom in M_2H_2 and a H atom in NH_3 are close to each other before the reaction (top row), the N atom and two H atoms which make a H_2 dimer line up almost linearly at the energy maximum (middle row), and the H_2 dimer exists near the M_2HNH_2 cluster, in which NH_2 exists between two M atoms, after the reaction (bottom row). Throughout the reaction, the H atom in M_2H_2 which does not make a H_2 dimer is apart from NH_3 or NH_2.

These results indicate that the reactions of each M_2H_2 cluster and NH_3 take structurally similar process irrespective of M, and that we should discuss the quantitative differences of these three systems to clarify the M dependence of the reaction processes.

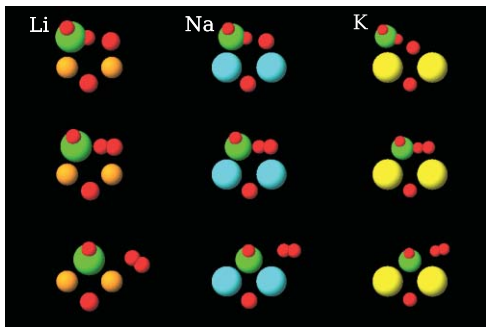

FIG. 3. Snapshots of the reaction processes of M_2H_2 with NH_3. The left, center, and right columns correspond to atomic configurations for M = Li, Na, and K, respectively. The top, middle, and bottom rows show the atomic configurations corresponding to those of the energy minimum before the reaction (M_2H_2–NH_3), the energy maximum during the reaction (transition state), and the energy minimum after the reaction (M_2HNH_2–H_2), respectively.

2. Potential energies of each state

In Fig. 4 we show the potential energies of each state during the reaction of M_2H_2 with NH_3. Black, red, and blue lines show the potential energies for M = Li, Na, and

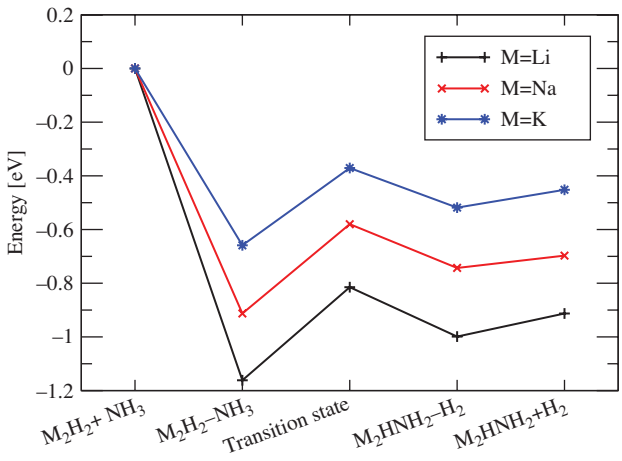

FIG. 4. Potential energies of each state during the reaction of M_2H_2 with NH_3: from left to right, the sum of the energies of an isolated M_2H_2 cluster and an isolated NH_3 molecule (M_2H_2+NH_3), the energy minimum before the reaction (M_2H_2–NH_3), the energy maximum during the reaction (transition state), the energy minimum after the reaction (M_2HNH_2–H_2), and the sum of the energies of an isolated M_2HNH_2 cluster and an isolated H_2 molecule (M_2HNH_2+H_2), respectively.

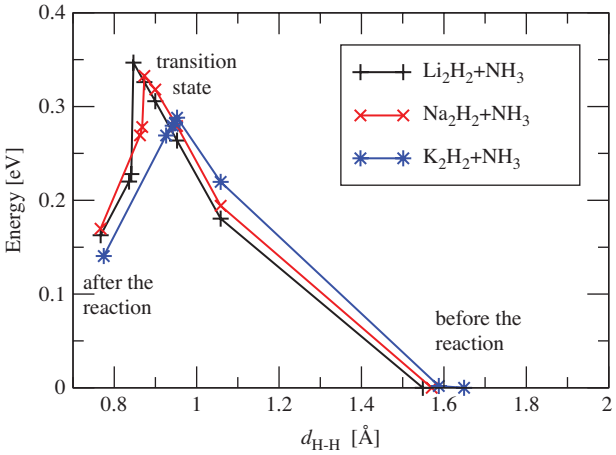

FIG. 5. H–H distance (d_{H-H}) dependence of the potential energies of the M_2H_2+NH_3 system. The right side of the figure corresponds to the states with the energy minima before the reaction (M_2H_2–NH_3 in Fig. 4, these energies are taken as the origin of the energy), the maximum points of the energies correspond to the transition state in Fig. 4, and the left side of the figure corresponds to the states with the energy minima after the reaction (M_2HNH_2–H_2 in Fig. 4).

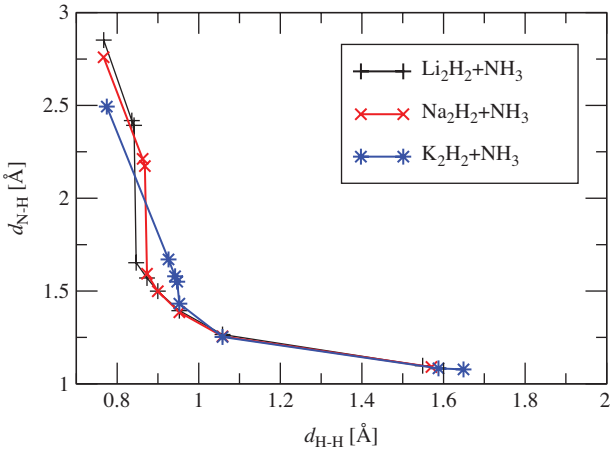

FIG. 6. H–H distance (d_{H-H}) dependence of the N–H distance in NH_3 (d_{N-H}).

K, respectively. The abscissa shows, from left to right, the six states for which the potential energies are calculated, i.e., the sum of the energies of an isolated M_2H_2 cluster and an isolated NH_3 molecule (M_2H_2+NH_3), the energy minimum before the reaction (M_2H_2–NH_3), the energy maximum during the reaction (transition state), the energy minimum after the reaction (M_2HNH_2–H_2), and the sum of the energies of an isolated M_2HNH_2 cluster and an isolated H_2 molecule (M_2HNH_2+H_2), respectively. We take the energy of M_2H_2+NH_3 as the origin of the energy.

From Fig. 4 we can see, by comparing the energies of M_2H_2+NH_3 and M_2HNH_2+H_2, that the energies for all cases decrease due to these reactions, that is, the reactions are exothermic. We can also see that the absolute values of the energy change decrease in order of M = Li, Na, and K, and that the M dependence of the energy change is clearly seen in the adsorption processes of NH_3 on M_2H_2 (M_2H_2+NH_3 → M_2H_2–NH_3), while the M dependence of the energy change in the remaining processes (M_2H_2–NH_3 → M_2HNH_2+H_2) is relatively small.

The energy change for M = Li is estimated to be about 0.91 eV and this value is about twice of the enthalpy change estimated from the experiment (50 kJ/mol,[5] corresponding to 0.52 eV). One of the reasons for the difference between the experiment and this calculation is that the enthalpy change estimated from the experiments is that of the system at finite temperature, in which both MH before the reaction and MNH_2 after the reaction are bulk,

$$\mathrm{MH(bulk)} + \mathrm{NH_3(gas)} = \mathrm{MNH_2(bulk)} + \mathrm{H_2(gas)} + \Delta H, \tag{4}$$

while Fig. 4 shows the energy change of the system at the temperature of 0 K, in which M_2H_2 cluster becomes M_2HNH_2 cluster by the reaction

$$\mathrm{M_2H_2(cluster)} + \mathrm{NH_3(molecule)} = \mathrm{M_2HNH_2(cluster)} + \mathrm{H_2(molecule)} + \Delta E, \tag{5}$$

and ΔH in Eq. (4) and ΔE in Eq. (5) should not be compared directly, though the energy change in the H_2 desorption from Li_1H_1 with NH_3 by the previous study[13] is 43.8–54.6 kJ/mol (0.454–0.566 eV) and similar to the experimental result (50 kJ/mol).[5]

3. Potential barrier

According to Fig. 4, the energy maxima of the systems during the reaction are lower than the energy of the initial states (M_2H_2+NH_3). However, it does not mean that the reactions occur freely.

Since, according to the present method of calculation, the energy needed to climb the potential barrier (M_2H_2–NH_3 → transition state) is the energy related to only one degree of freedom (d_{H-H}, the distance between two H atoms which form a H_2 dimer), the kinetic energy generated by the exothermic reaction of the NH_3 adsorption (M_2H_2+NH_3 → M_2H_2–NH_3) diffuses over the whole system. The present small system has 18 degrees of freedom (there are six free atoms, while the positions of two Li atoms are fixed), and the contribution of the adsorption energy of NH_3 is only about 0.05 eV for

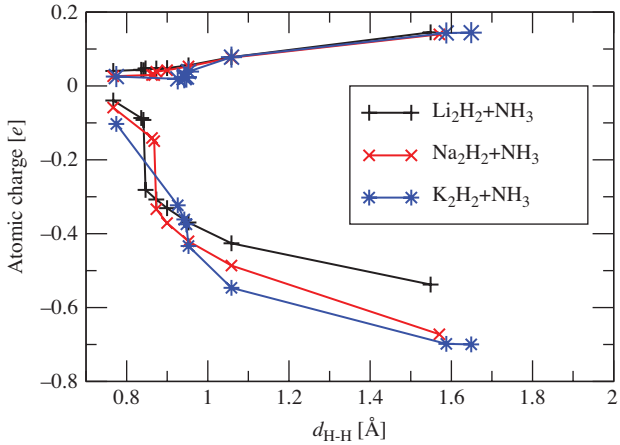

FIG. 7. H–H distance (d_{H-H}) dependence of the atomic charges of N, H in NH_3 and H in M_2H_2.

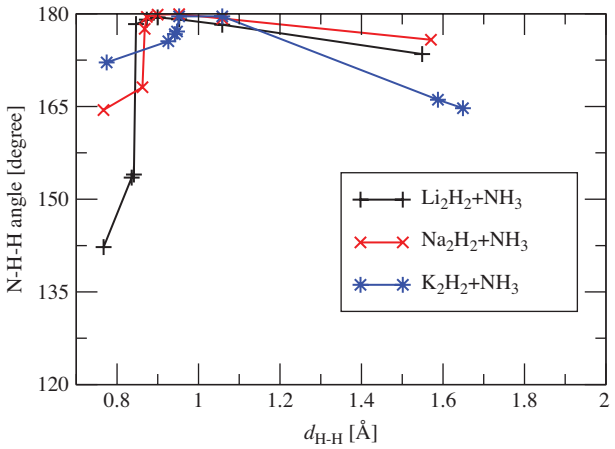

FIG. 8. H–H distance (d_{H-H}) dependence of the N–H–H angle.

each degree of freedom. On the other hand, the distribution of the instantaneous energy ϵ distributed to a degree of freedom is proportional to

$$\exp(-\epsilon/k_B T_0), \tag{6}$$

where k_B is the Boltzmann constant and T_0 is the temperature of the system, and a degree of freedom can take energies higher than $k_B T_0$. This is why a reaction with an activation energy much higher than room temperature (for example, the activation energy of 0.5 eV corresponds to about 5000 K) proceeds at room temperature during a few minutes to hours. To discuss the potential barrier of the reaction, it is convenient to choose the energy minima before the reaction (M_2H_2–NH_3) as the origin of the energy.

During the reaction process of M_2H_2 with NH_3, we decrease the distance between a H atom in M_2H_2 and a H atom in NH_3 (d_{H-H}) to form a H_2 dimer. In Fig. 5 we show the d_{H-H} dependence of the potential energies of the M_2H_2+NH_3 system. Black, red, and blue lines show the potential energies for M = Li, Na, and K, respectively. The states for $d_{H-H} \simeq 1.6$ Å (right side of the figure) correspond to the states with the energy minima before the reaction (M_2H_2–NH_3 in Fig. 4, these energies are taken as the origin of the energies in Fig. 5), the maximum points of the energies correspond to the transition states in Fig. 4, and the states for $d_{H-H} \simeq 0.8$ Å (left side of the figure) correspond to the states with the energy minima after the reaction (M_2HNH_2–H_2 in Fig. 4).

From Fig. 5, we can see that the potential energies at the transition states for M = Li, Na, and K are 0.346, 0.332, and 0.282 eV, respectively, and d_{H-H} at the transition states are 0.846, 0.873, and 0.953 Å, respectively. That is, the potential barriers become lower in height and take larger distance in order of Li, Na, and K. We have also estimated the potential energy maximum with nudged elastic band method.[27] The estimated energies are 0.336, 0.329, and 0.290 eV, respectively, and these values are similar to those with the present method. We can also see that, after the system goes over the transition state, the energy sharply decreases for Li, and the decreases of the energy become slower in order of Na and K.

The differences of the heights of the potential barrier are consistent with the M dependence of the reaction yields estimated by the experiment [53%, 60%, and 100% for M = Li, Na, and K, respectively (Ref. 8)]. It is also consistent with the experimental results that the difference of the heights, position, and softness of the potential barrier between Na and K is larger than that between Li and Na.

We can regard that the difference of the potential barrier comes from the absolute value of the Coulomb energy between M^+ ion and the outermost electron in M atom, i.e., the first ionization energy, which decreases in order of Li, Na, and K since the distance between M^+ and the outermost electron increases in order of Li, Na, and K. With decrease in the first ionization energy, the outermost electron in M atom can easily move to H atom in MH. Since $H^{\delta-}$ in MH and $H^{\delta+}$ in NH_3 make a dimer, i.e., the negative charge of $H^{\delta-}$ moves to $H^{\delta+}$, it is favorable if $H^{\delta-}$ has more electron. As we can see in Sec. III A 4, the absolute value of the charge of $H^{\delta-}$ in MH increases in order of Li, Na, and K, while there is little difference in the charge of $H^{\delta+}$ and N–H distance in NH_3.

Here we compare our results with those of MNH_2BH_3 and MBH_4. For MNH_2BH_3, Kim *et al.*[14] show, by high level *ab initio* calculations, that the energy barrier of the dehydrogenation process of $(NaNH_2BH_3)_2$ is lower than that of $(LiNH_2BH_3)_2$, consistent with the experimental result.[9] Since the dominant dehydrogenation process of MNH_2BH_3 is predicted to be the metal mediated pathway, i.e., dehydrogenation through M-$H^{\delta-}$ and N–$H^{\delta+}$,[14,33] these results are consistent with our results for MH + NH_3. However, they also

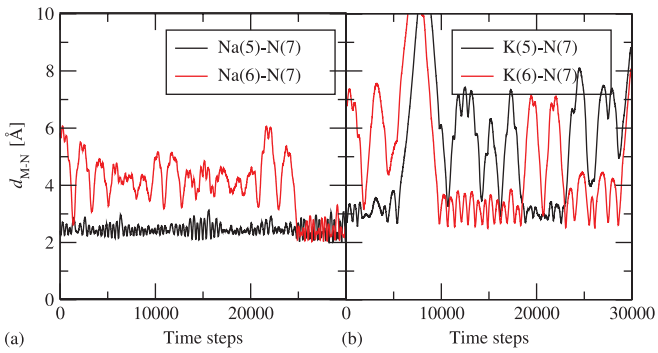

FIG. 9. Time evolution of the M–N distance (d_{M-N}) at 700 K for (a) M = Na and for (b) M = K.

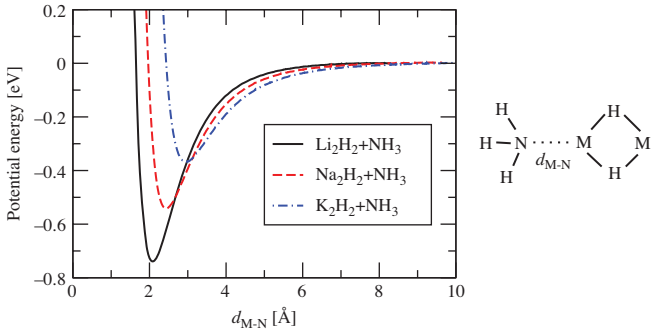

FIG. 10. Potential energy of the system of the M_2H_2+NH_3 system. The abscissa shows the M–N distance (d_{M-N}). During the calculation, two M atoms and a N atom line up linearly and the shape of the M_2H_2 cluster and the NH_3 molecule are fixed.

predicted that the energy barrier of the dehydrogenation process of $(KNH_2BH_3)_2$ is higher than that of $(LiNH_2BH_3)_2$, inconsistent with our results. The recent experiment shows that the structure of KNH_2BH_3 differs substantially from those of $LiNH_2BH_3$ and $NaNH_2BH_3$.[34] This structural difference may break the order of the M dependence of the reactivity.

It is not strange that the reactivity of MBH_4 decreases in order of Li > Na > K and we can interpret this tendency in the same ways as our results. Since the electronegativity of B is smaller than that of H and all the hydrogen atoms in MBH_4 should be negatively charged, the absolute value of charge of $H^{\delta-}$ should increase in order of Li < Na < K. The repulsion between $H^{\delta-}$ atoms increases and the reactivity should decrease in order of Li > Na > K.

4. Atomic configurations and atomic charges

In Figs. 6 and 7 we show the d_{H-H} dependence of the N–H distance in NH_3 (d_{N-H}) and that of the atomic charges of N, H in NH_3 and H in M_2H_2, respectively. Black, red, and blue lines show the quantities for M = Li, Na, and K, respectively. From these figures, we can see that, before the system goes over the transition state, there are almost no M dependence in d_{N-H} and in the charge of H in NH_3, while the absolute values of the charge of H in M_2H_2 increases in order of Li, Na, and K. These results indicate that the difference of M does not affect NH_3 significantly before the system goes over the transition state, while the difference affects the atomic charges of M_2H_2 as expected from the electronegativities (the electronegativities of Li, Na, K, N, and H are 0.98, 0.93, 0.82, 3.04, and 2.20, respectively[35]). After the system goes over the transition state, the changes of the interatomic distances and atomic charges become softer in order of Li, Na, and K, as seen in the potential barriers.

In Fig. 8 we show the d_{H-H} dependence of the N–H–H (N in NH_3, H in NH_3, H in M_2H_2) angles. Black, red, and blue lines show the angles for M = Li, Na, and K, respectively. In each case, we can see that the N–H–H angle is almost 180° around the d_{H-H} where the reaction occurs. Since H in MH has negative charge and H in NH_3 has positive charge, we can regard that $N^{\delta-}$–$H^{\delta+}_{NH_3}$–$H^{\delta-}_{MH}$ ions line up linearly to minimize the Coulomb energy among these ions by making $N^{\delta-}$ and $H^{\delta-}$ apart from each other.

B. Reaction process by molecular dynamics simulation

1. Reaction of M_2H_2 with NH_3

Among the present three systems, the Li_2H_2–NH_3 system was already shown to desorb a H_2 molecule by the MD simulations at temperatures of 700 and 1000 K within 14.4 ps.[12] In this paper, we have tried to reproduce the H_2 desorption from M_2H_2 (M = Na and K) and NH_3 at the same condition as that for M = Li to investigate the M dependence of the dynamics.

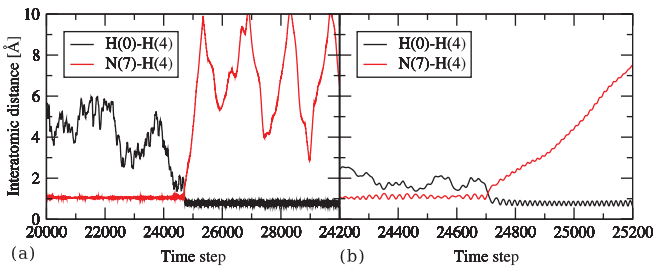

FIG. 11. Time evolution of the interatomic distances of the Na_2H_2+NH_3 system at 700 K for (a) 20 000–30 000 steps and (b) around the reaction (24 200–25 200 steps).

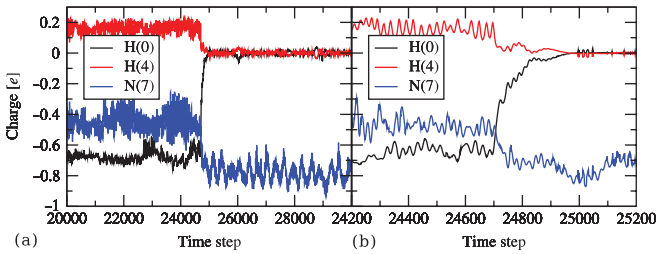

FIG. 12. Time evolution of the atomic charges of the Na_2H_2+NH_3 system at 700 K for (a) 20 000–30 000 steps and (b) around the reaction (24 200–25 200 steps).

In Table I we show the results for the H_2 desorption from the M_2H_2+NH_3 system. For the simulations with M = Na, we succeeded to reproduce the H_2 desorption at 700 K, while the H_2 desorption did not occur at 1000 K within 14.4 ps. For the simulations with M = K, the H_2 desorption did not occur both at 700 and 1000 K within 14.4 ps. At a glance, these results conflict with the experimental results (the reaction yields are 53%, 60%, and 100% for M = Li, Na, and K, respectively [8]). The origin of this discrepancy can be understood as follows.

We have noticed from our simulations that, when the H_2 desorption does not occur, NH_3 does not stay on an M atom. In Fig. 9 we show the time evolution of the M–N distances ($d_{M–N}$) at 700 K for (a) M = Na and for (b) M = K. While the N atom always stays on the Na(5) atom before the reaction for M = Na, the N atom does not always stay on a K atom for M = K and moves to another K atom and goes away from the K_2H_2 cluster. For M = Na at 1000 K, the N atom also does not stay on a Na atom and goes away from the Na_2H_2 cluster. If the NH_3 molecule stays on an M atom only for a very short time, it is difficult for H in NH_3 and H in M_2H_2 to get close to each other, and, therefore, the chance of the H_2 dimer formation decreases. These problems may be caused by the present simplified small system at high temperature and within short time (14.4 ps), which does not correspond to the real complex system directly.

The reason why NH_3 can easily go away from the M_2H_2 cluster for M = Na and K is, as we can see from Fig. 4, that the adsorption energy of NH_3 to M_2H_2 becomes smaller in order of Li, Na, and K. While the absolute values of the charges of M and H in M_2H_2 become larger in order of Li, Na, and K, the radius of M atom increases in order of Li, Na, and K. In Fig. 10 we show the potential energy of the M_2H_2 + NH_3 system as a function of $d_{M–N}$. Note that two M atoms and a N atom line up linearly and we change only $d_{M–N}$ (the shape of the M_2H_2 cluster and the NH_3 molecule are not changed), so the potential energy shown in Fig. 10 is different from that shown in Fig. 4. From Fig. 10, we can see that $d_{M–N}$ at the energy minimum of the M_2H_2+NH_3 system shifts to larger distance and the depth of the energy minimum gets shallower in order of M = Li, Na, and K.

TABLE I. Hydrogen desorption from M_2H_2–NH_3 systems.

System	700 K	1000 K
Li_2H_2–NH_3	Yes[a]	Yes[a]
Na_2H_2–NH_3	Yes	No
K_2H_2–NH_3	No	No

[a]The results for the Li_2H_2–NH_3 system are from the previous study (Ref. 12).

2. Time evolution

In Figs. 11 and 12 we show the time evolutions of the interatomic distances and the atomic charges, respectively, of the Na_2H_2+NH_3 system at 700 K. From Fig. 11 we can see that the H_2 dimer is formed at about 24 720 steps. On the other hand, from Fig. 12 we can see that the charges of the H atoms which make the dimer are $0.15e$ to $0.2e$ for H in NH_3, and $-0.6e$ to $-0.7e$ for H in M_2H_2 before the reaction. These H atoms get close to neutral when the H_2 dimer is formed, but each H atom still has a finite charge, and both H atoms become almost neutral at about 24 970 steps, a few hundred time steps after the occurrence of the dimerization. This tendency is same as that of the Li_2H_2+NH_3 system.[12]

IV. SUMMARY

In this paper, we have studied the M dependence of the reactivity of MH (M = Li, Na, and K) with NH_3 by calculating the potential barrier of the H_2 desorption from the M_2H_2+NH_3 system. We have shown that the height of the potential barrier becomes lower in order of Li, Na, and K, where the difference in Li and Na is relatively smaller compared with that in Na and K, and this tendency is consistent with the experimental results. We have also shown that the H–H distance at the transition state takes larger distance and the change of the potential energy around the energy maximum becomes softer in order of Li, Na, and K. There is almost no M dependence in the charge of H atom in NH_3, while that of the H atom in M_2H_2 takes larger negative value in order of Li, Na, and K.

We have also performed *ab initio* MD simulations on the M_2H_2–NH_3 systems (M = Na and K) and succeeded to reproduce the H_2 desorption from the Na_2H_2–NH_3 system, while we could not reproduce the H_2 desorption from the K_2H_2–NH_3 system. We have shown that these results can be understood by the M dependence of the adsorption energy of NH_3 on M_2H_2.

ACKNOWLEDGMENTS

This work is supported by the grants of the NEDO project "Advanced Fundamental Research on Hydrogen Storage Materials" in Japan. Most of the computation in this work was performed by supercomputer at Research Institute for Information Technology, Kyushu University.

[1] J. Graetz, Chem. Soc. Rev. **38**, 73 (2009).
[2] S. A. Shevlin and Z. X. Guo, Chem. Soc. Rev. **38**, 211 (2009).
[3] P. Chen, Z. T. Xiong, J. Z. Luo, J. Y. Lin, and K. L. Tan, Nature (London) **420**, 302 (2002).
[4] T. Ichikawa, N. Hanada, S. Isobe, H. Y. Leng, and H. Fujii, J. Phys. Chem. B **108**, 7887 (2004).
[5] S. Hino, N. Ogita, M. Udagawa, T. Ichikawa, and Y. Kojima, J. Appl. Phys. **105**, 023527 (2009).
[6] Y. H. Hu and E. Ruckenstein, J. Phys. Chem. A **107**, 9737 (2003).
[7] Y. Kojima, K. Tange, S. Hino, S. Isobe, M. Tsubota, K. Nakamura, M. Nakatake, H. Miyaoka, H. Yamamoto, and T. Ichikawa, J. Mater. Res. **24**, 2185 (2009).
[8] H. Yamamoto, H. Miyaoka, S. Hino, H. Nakanishi, T. Ichikawa, and Y. Kojima, Int. J. Hydrogen Energy **34**, 9760 (2009).
[9] Z. Xiong, C. K. Yong, G. Wu, P. Chen, W. Shaw, A. Karkamkar, T. Autrey, M. O. Jones, S. R. Johnson, P. P. Edwards, and W. I. David, Nature Mater. **7**, 138 (2008).
[10] A. Züttel, P. Wenger, S. Rentsch, P. Sudan, Ph. Mauron, and Ch. Emmenegger, J. Power Sources **118**, 1 (2003).
[11] Y. Nakamori, K. Miwa, A. Ninomiya, H. Li, N. Ohba, S. Towata, A. Züttel, and S. Orimo, Phys. Rev. B **74**, 045126 (2006).
[12] A. Yamane, F. Shimojo, K. Hoshino, T. Ichikawa, and Y. Kojima, J. Mol. Struct.: THEOCHEM **944**, 137 (2010).
[13] T. Kar, S. Scheiner, and L. Li, J. Mol. Struct.: THEOCHEM **857**, 111 (2008).
[14] D. Y. Kim, N. J. Singh, H. M. Lee, and K. S. Kim, Chem.-Eur. J. **15**, 5598 (2009).
[15] S. Isobe, T. Ichikawa, S. Hino, and H. Fujii, J. Phys. Chem. B **109**, 14855 (2005).
[16] P. Hohenberg and W. Kohn, Phys. Rev. **136**, B864 (1964).
[17] W. Kohn and L. J. Sham, Phys. Rev. **140**, A1133 (1965).
[18] M. P. Teter, M. C. Payne, and D. C. Allan, Phys. Rev. B **40**, 12255 (1989).
[19] T. A. Arias, M. C. Payne, and J. D. Joannopoulos, Phys. Rev. B **45**, 1538 (1992).
[20] T. A. Arias, M. C. Payne, and J. D. Joannopoulos, Phys. Rev. Lett. **69**, 1077 (1992).
[21] G. Kresse and J. Hafner, Phys. Rev. B **49**, 14251 (1994).
[22] F. Shimojo, Y. Zempo, K. Hoshino, and M. Watabe, Phys. Rev. B **52**, 9320 (1995).
[23] J. P. Perdew, K. Burke, and M. Ernzerhof, Phys. Rev. Lett. **77**, 3865 (1996).
[24] P. E. Blöchl, Phys. Rev. B **50**, 17953 (1994).
[25] G. Kresse and D. Joubert, Phys. Rev. B **59**, 1758 (1999).
[26] R. S. Mulliken, J. Chem. Phys. **23**, 1833 (1955).
[27] H. Jonsson, G. Mills, and K. W. Jacobsen, "Nudged elastic band method for finding minimum energy paths of transitions," in *Classical and Quantum Dynamics in Condensed Phase Simulations*, edited by B. J. Berne, G. Ciccotti, and D. F. Coker (World Scientific, Singapore, 1998), p. 385.
[28] S. Nosé, Mol. Phys. **52**, 255 (1984).
[29] S. Nosé, J. Chem. Phys. **81**, 511 (1984).
[30] W. G. Hoover, Phys. Rev. A **31**, 1695 (1985).
[31] G. Libowitz, J. Nucl. Mater. **2**, 1 (1960).
[32] J. G.O. Ojwang, R. van Santen, G. J. Kramer, A. C.T. van Duin, and W. A. Goddard, J. Chem. Phys. **128**, 164714 (2008).
[33] D. Y. Kim, H. M. Lee, J. Seo, S. K. Shin, and K. S. Kim, Phys. Chem. Chem. Phys. **12**, 5446 (2010).
[34] H. V. K. Diyabalanage, T. Nakagawa, R. P. Shrestha, T. A. Semelsberger, B. L. Davis, B. L. Scott, A. K. Burrell, W. I. F. David, K. R. Ryan, M. O. Jones, and P. P. Edwards, J. Am. Chem. Soc. **132**, 11836 (2010).
[35] L. Pauling, *The Nature of the Chemical Bond*, 3rd ed. (Cornell University Press, USA, 1960).